Pergamon

Bioorganic & Medicinal Chemistry 7 (1999) 161–175

BIOORGANIC & MEDICINAL CHEMISTRY

Synthesis and Study of Peptides with Semirigid i and i + 7 Side-chain Bridges Designed for α-Helix Stabilization

Chongxi Yu and John W. Taylor*

Rutgers University, Department of Chemistry, Piscataway, NJ 08855, USA

Received 2 June 1998; accepted 13 October 1998

Abstract—A search for conformational constraints on the peptide α-helical conformation indicated that *para*-substituted amino acid derivatives of a benzene ring might be suitable for linking pairs of side chains that are separated by two turns of the helix. A 14-residue synthetic, amphiphilic α-helical peptide model system has been used to study the helix stabilizing effects of a series of four such bridges having constitutionally isomeric structures. These bridges were used to link positions 3 and 10 of the model peptides. The peptides were synthesized in good yield by standard solid-phase methods, including cyclization on the solid support. They were then studied for their solution conformations and melting behavior by circular dichroism (CD) spectropolarimetry, and for their elution behavior on reversed-phase HPLC columns. In aqueous solution and in 50% (v/v) trifluoroethanol, the most effective bridge for helix stabilization consisted of a 4-(aminomethyl)phenylacetic acid residue (AMPA) linked by amide bonds to the side chain functional groups of a (*S*)-2,3-diaminopropionic acid residue (Dap) in position 3 of the model peptide and an aspartic acid residue in position 10. This Dap^{3}(AMPA), Asp^{10} bridge was about as effective as two Lys^{i}, Asp^{i+4} lactam bridges incorporated linking residues 3 and 7, and 10 and 14, in the same model peptide sequence. This suggests that it is worth about 1 kcal/mol of helix stabilization energy. © 1999 Elsevier Science Ltd. All rights reserved.

Introduction

The incorporation of elements of cyclic structure into biologically active peptides has long been used as a means of conformational constraint. Studying the effects of cyclic constraints on the conformational properties of a peptide, in parallel with assays of the biological activities of such analogues, has often led to detailed insights into the active conformations of flexible peptide ligands at receptor sites. Since many ligand–receptor complexes are inaccessible to direct structural determinations, such detailed indirect information is essential to enable the rational design of peptidomimetics that might have advantageous properties compared to the native peptides, including increased potencies and/or bioavailabilities, or altered receptor specificities or agonist–antagonist character.

A variety of peptide and protein ligands, including the amphiphilic α-helical peptide hormones,[1,2] and DNA-binding proteins in the b-zip and b-HLH classes,[3] contain within their structures short peptide sequences that are either known or hypothesized to adopt an α-helical conformation upon binding to their respective receptor surfaces. However, the unbound ligands in solution are usually observed to have little helical structure in the same sequences, because of the marginal stability of the α-helical conformation in the absence of stabilizing interactions. For small flexible, linear peptides, the entropic cost of folding just the peptide backbone into the unique α-helical conformation required for receptor recognition is high. For example, the conformational entropy calculated for folding a small, linear protein into a compact globule is at least −1.0 to 1.4 cal/K per mol of residues, without consideration of secondary structure formation or side-chain constraints.[4] Therefore, in addition to defining the active conformations of such peptides, the introduction of cyclic constraints that greatly reduce the flexibility of the peptide backbone in favor of α-helix formation, should result in a significant increase in their affinities for their receptors.

The linking, through covalent chemical bonds, of amino acid side chains that are adjacent to one another on the surface of an α-helix is one approach to achieving the parallel goals of both defining the functional importance of an α-helical structure and enhancing its receptor affinity. For this purpose, several side-chain to side-chain bridging structures have been proposed and explored, although they have rarely been compared to one another for their helix stabilizing properties in a systematic fashion. Historically, the first approach of this type, introduced by Felix and co-workers in their studies of growth-hormone releasing factor (GRF)

Key words: Amino acids and derivs; peptides and polypeptides; solid-phase synthesis; mimetics; proteins.
*Corresponding author. Tel: +1 732 445 0514; Fax: +1 732 445 5312.

0968-0896/99/$ - see front matter © 1999 Elsevier Science Ltd. All rights reserved.
PII: S0968-0896(98)00232-6

analogues,[5] was to link the side chains of lysine and aspartic acid residues separated by three intervening residues in the linear sequence (the *i*th, and the [i + 4]-th residues) by formation of a bridging, cyclic amide (lactam) bond. GRF analogues with lactam bridges linking a Lys^{i}, Asp^{i} pair, or the reversed Asp^{i}, Lys^{i+4} pair, were both reported to have higher helical contents than their parent peptides, as judged by circular dichroism (CD) and ^{1}H NMR spectroscopy. Subsequently, this i, i + 4 type of lactam bridge has been used to investigate structure–activity relationships in a number of other amphiphilic α-helical peptide hormones in addition to GRF, including calcitonin,[6] parathyroid hormone,[7] and neuropeptide Y.[8] These studies have demonstrated the potential utility of side-chain lactam cyclizations to enhance the potency of a peptide ligand in vitro and in vivo. However, the clearest relationship between helix stabilization by Lys^{i}, Asp^{i+4} lactam bridges and receptor affinity has been established in studies of DNA-binding by bridged analogues of the basic region of the yeast transcription factor, GCN4,[9,10] since the formation of an α-helical conformation upon receptor (DNA) binding had been directly established only for this example. In this case, the N-terminal and C-terminal (i, i + 4)-bridged structures introduced into the GCN4 basic region enhanced both the helix stability (assuming a two-state coil–helix equilibrium) and the GCN4 peptide affinity for its specific DNA recognition site by about 0.2 kcal/mol and 0.5 kcal/mol, respectively, and by about 1 kcal/mol in combination.[10]

Given the relatively small stabilizing effects of individual Lys^{i}, Asp^{i+4} side-chain lactam bridges, it is not surprising that their effects on helix stability have been found to depend on the amino acid sequence context of the bridge. The CD spectra determined for lactam-bridged calcitonin analogues[6] illustrate that the helical propensities[11] of the amino acid residues substituted by the bridging Lys/Asp pair will, naturally, have a significant affect on the degree of helix stabilization observed. Similarly, a study of Lys^{i}, Asp^{i+4} lactam-bridged analogues of the second transmembrane domain proposed for the δ-opioid receptor[12] has shown that the identity of the three residues in the intervening positions between the bridged pair determines helix stability in the same rank order as it would in a linear peptide sequence. Finally, again assuming a two-state coil–helix equilibrium, the logarithmic relationship between helix content and the free energy change associated with helix formation means that a helix stabilizing effect of the order of 0.5 kcal/mol will result in little observable helix formation in peptide sequences that only have a marginal tendency to adopt the α-helical conformation to begin with (Fig. 1).

In order to evaluate the helix-stabilizing effects of a variety of alternatives to the Lys^{i}, Asp^{i+4} and Asp^{i}, Lys^{i+4} lactam bridges, we have developed a model peptide system illustrated by the dicyclic Lys/Asp bridged analogue, peptide 2-2, shown in Figure 2.[13,14] Since this peptide has a ΔG value close to zero for the coil–helix equilibrium, the CD spectra of analogues incorporating alternative bridging structures are sensitive to

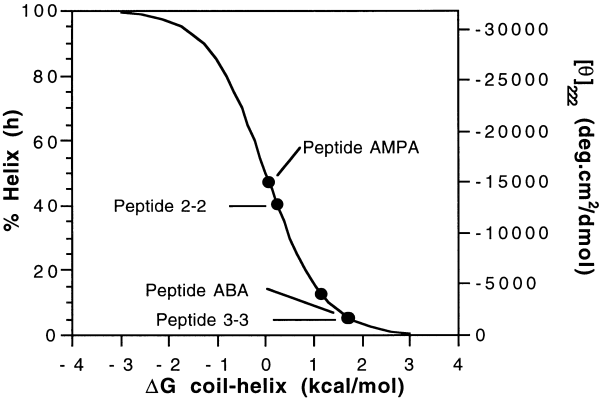

Figure 1. Relationship between the peptide helicity measured from the CD spectrum and ΔG for the coil–helix equilibrium. The mean residue ellipticity, [θ], at 222 nm is used to estimate % helix for 14-residue peptides as described in the text.[23] Percent helix, h, is related to the free energy for the coil–helix equilibrium, assuming a single-step, cooperative transition, by the equation $\Delta G = -RT \ln\{h/(100\,h)\}$, for T = 298 K. Experimental values for certain peptide studies reported here are also indicated (see results).

differences in their helix stabilizing effects (Fig. 1). Within this constant peptide sequence context, several closely related side-chain bridging structures have been compared to the Lys^{i}, Asp^{i+4} bridges for their helix stabilizing effects. All of these modified structures have been found to result in less helical structure than that found for peptide 2-2.[12] The bridges tested included Orn^{i}, Glu^{i+4} bridges, Lys^{i}, Glu^{i+4} bridges, and γ-thio-Lys^{i}, Asp^{i+4} bridges, in which the γ methylene group in the lysine side chain is substituted by a sulfur atom. However, residue pairs in positions i and i + 3 in the linear sequence are also adjacent on the helix surface. Van't Hoff analysis of the effects of incorporating two Asp^{i}, Lys^{i+3} side-chain lactam bridges into an apolipoprotein E peptide[15] indicated that these bridges together resulted in a total of about 1 kcal/mol of helix stabilization, and that this stabilizing effect was entirely entropic, as expected. This (i, i + 3)-bridge is, therefore, about as effective for helix stabilization as the Lys^{i}, Asp^{i+4} bridges. Furthermore, the incorporation of two Lys^{i}, Asp^{i+4} bridges into overlapping positions in a peptide sequence has been shown to result in dramatically stabilized, short α-helical structures that are highly resistant to thermal denaturation.[16,17]

Helical peptides that are involved in molecular recognition are likely to have several essential amino acid residues displayed on the helix surface in a variety of patterns. Therefore, in order to explore helix function in biological systems, and to produce rigid helices as peptidomimetic scaffolds of more general applicability as ligands, it is essential to develop several alternative helix stabilizing side-chain bridging structures having different linking points in the linear sequence. Since the *i*th and the (i + 7)-th residues in a linear sequence are also on proximal positions on the surface of an α helix, but separated by two turns of the helix rather than one, side-chain bridges designed to link residue pairs with this spacing have also been developed. Jackson et al.[18] have shown that effective helix stabilization is attained

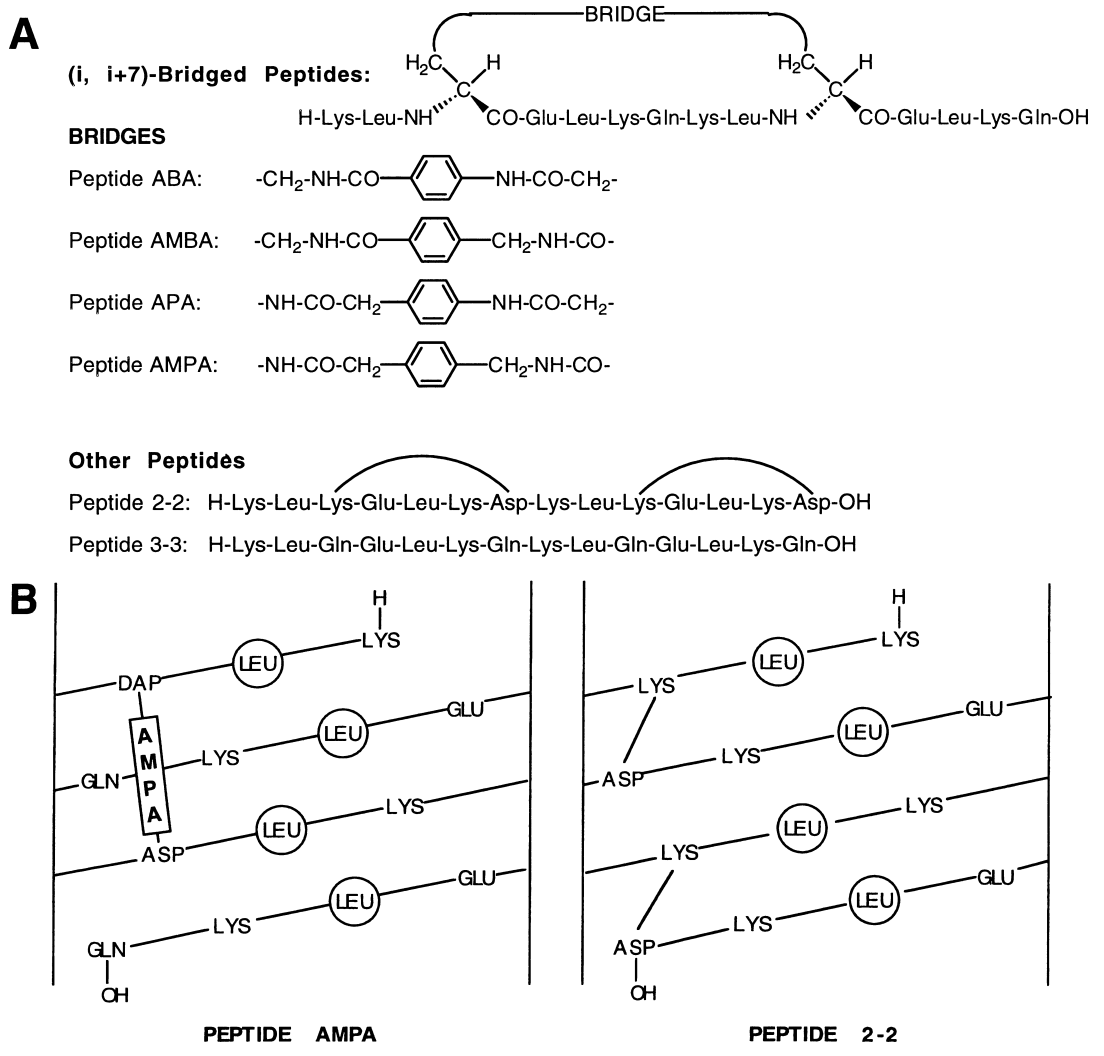

Figure 2. Model peptide structures. (A) The primary structures and side-chain bridging structures of all of the model peptide structures described in this study are shown. (B) Helical net diagrams of the synthetic model amphiphilic α-helical peptides, peptide AMPA and peptide 2-2, are compared. The hydrophobic residues are circled, and both backbone and side-chain bridging amide bond connections are indicated by sloping solid lines.

using a disulfide link to connect a D-thiolysine residue (with a thiol-functionalized side chain instead of the ε-amine) in the N-terminal, *i*th position to the corresponding L-thiolysine residue placed in the C-terminal (i + 7)-th position. This bridge design takes advantage of the fact that the C^{α}–C^{β} side-chain bonds in the bridging N-terminal D-amino acid and C-terminal L-amino acid residues will be oriented towards each other, simplifying the design of a linking structure needed to connect them. However, this bridge retains considerable freedom of motion on the helix surface, due to the eight methylene groups in the link, and might be further optimized for helix formation by the incorporation of more rigid structural features. Also, D-amino acid residues are known to destabilize α-helices by about 1 kcal/mol,[19] and helix-disrupting effects of the N-terminal D-thiolysine bridging residue were reported for a monocyclic apamin-derived peptide in which this bridge was used.[20] Finally, disulfide linkages as constraints for reporting effects on biological activities are limited by the possibility that disulfide exchange reactions in vivo may occur, limiting the applicability of this bridge design.

One alternative to the thiolysine (i, i + 7)-disulfide bridge that was reported recently by Phelan et al.,[20] investigated the side-chain linkage of (i, i + 7)-spaced glutamic acid residues by amide-bond formation with 1,3-diaminopropane. This bridge, placed into positions 3 and 10 of an N^{α}-acetylated 13-residue alanine-rich model peptide amide generated a highly helical structure, which was characterized by ^{1}H NMR and CD as more helical[20] than a monocyclic apamin analogue bridged by the D- and L-thiolysine link of Jackson et al.[18] We have also been exploring alternative i, i + 7 helix-stabilizing bridge designs,[21] but our approach has been to search for relatively rigid linking structures, rather than flexible methylene chains, to connect two (i, i + 7)-spaced L-amino acid residues with amide bonds. Here we report on the synthesis and solution conformational studies of a series of four monocyclic peptide analogues (shown in Fig. 2) that incorporate isomeric bridging structures based on *para*-substituted benzene rings into residue positions three and ten of the same model peptide sequence as that of peptide 2-2 (Fig. 2). The most effective of these four bridging isomers consists of a 1,2-diaminopropionic acid residue (Dap) in position 3 linked

via a *p*-(aminomethylphenyl)acetic acid residue (AMPA) to an aspartic acid residue in position 10. This bridge was reported previously to generate a highly rigid α-helical structure when used twice in a bicyclic analogue of peptide 2-2, in which it was incorporated into the overlapping 3-10 and 7-14 positions.[21] In this report, we show that just one Dap(AMPA)^3, Asp^{10} bridge (peptide AMPA, Fig. 2) is as effective for helix stabilization as the two Lys^i, Asp^{i+4} bridges in peptide 2-2. We also show that the other three isomeric bridge structures studied (Fig. 2A), in which the bridging amide bonds are moved into conjugation with the central, *para*-substituted benzene ring, are all less effective for helix stabilization.

Results

Peptide design

The design of the four monocyclic, (i, i+7)-bridged model peptides in this study (Fig. 2) is based on the amphiphilic α-helical model peptide series H-(cyclo$^{3\text{-}7}$[Lys-Leu-Lys-Glu-Leu-Lys-Asp])$_n$-OH, previously reported.[13,14] This repeat sequence generates a hydrophobic face composed of leucine side chains, and a hydrophilic face composed of lysine and glutamic acid residues. With positions 3 and 7 of the 7-residue repeat bridged, these model peptides have a net charge at neutral pH of +1 for each 7-residue repeat. We chose the 14-residue model peptide in this series, peptide 2-2 ($n=2$, Fig. 2), as our point of comparison, because this 14-residue peptide is about 40% α-helical in aqueous solution[13] and, therefore, CD measurements are optimally sensitive to differences in α-helix content relative to this peptide. It is important to note that, despite their amphiphilic character, the 7-, 14-, and 21-residue peptides in this model series are monomeric in aqueous solution, and that their α-helical structure does not, therefore, depend on intermolecular interactions.[13,14]

The i, i+7 side-chain bridges that we chose to examine for their α-helix stabilizing effects were designed by examination of space-filling Corey–Pauling–Koltun (CPK) molecular models, as well as computer modeling by geometry optimization of selected side-chain linking structures constrained to fit onto the C$^\alpha$ atoms of an i, i+7 residue pair on a fixed poly-Ala α-helix using the modeling software package HyperChem (AutoDesk, Inc.). These studies directed us towards *para*-substituted benzene rings with amide links to the i, i+7 residues on the helix. In order to maintain minimal flexibility in our bridging structure, we chose to explore four isomeric bridges in which the number of methylene groups necessary to link the *para*-substituted amide bonds on a benzene ring to the i, i+7 side chains was minimized at a total of four. In addition, for ease of synthesis and compatibility with peptide assembly using solid-phase methods, we considered only heterodifunctional, amino acid derivatives of benzene as linking structures, as opposed to possible homodifunctional, diamine, or dicarboxylic acid derivatives. The most rigid bridge of this type used amide bonds to link 4-aminobenzoic acid (ABA) to (*S*)-2,4-diaminobutyric acid (Dab) and Glu residues in positions 3 and 10, respectively, of the model peptide sequence (Fig. 2, peptide ABA). To facilitate comparisons of this monocyclic peptide with the bicyclic peptide 2-2, and the linear analogue, peptide 3-3 (Fig. 2), glutamine residues were used in the unbridged positions, 7 and 14, of peptide ABA, as an acyclic mimic of lactam-cyclized residues.

The other three model peptides in this study were also monocyclic, and had the same amino acid sequence as peptide ABA in the non-bridging positions, but had different isomeric bridges linking residues 3 and 10. In these bridges, conjugation of one or both of the amide bonds in the bridge with the benzene ring was broken by insertion of a methylene group taken from the side chain of Dab^3 or Glu^{10}, or both. In peptide APA, the methylene switch is made at the N-terminal end, so that an (*S*)-2,3-diaminopropionic acid residue (Dap) in position 3 is linked to Glu^{10} via the carboxyl function of a bridging 4-aminophenylacetic acid residue (APA); in peptide AMBA, the C-terminal methylene is switched, and Dab^3 is linked to an aspartic acid residue in position 10 via a bridging 4-(aminomethyl)benzoic acid residue (AMBA); and in peptide AMPA, Dap^3 is linked to Asp^{10} via a bridging 4-(aminomethyl)phenylacetic acid residue (AMPA), so that both bridging amides have the increased flexibility associated with the insertion of a methylene group between them and the benzene ring (Fig. 2).

Peptide synthesis

All four of the novel (i, i+7)-bridged, monocyclic peptides were synthesized using solid-phase methods based on Boc/benzyl chemistry, with side-chain to side-chain cyclization by lactam formation on the solid support, and using orthogonal Fmoc/OFm protection for the cyclized side-chain amine and carboxylic acid groups, as described by Felix et al.[5] The *para*-substituted benzene amino acid derivatives needed for the bridging structures in peptides ABA, APA, and AMBA were all commercially available in unprotected form, and were appropriately protected using standard methods. The *p*-(aminomethyl)phenylacetic acid needed for the synthesis of peptide AMPA was not commercially available, and was synthesized from *p*-(aminomethyl)benzoic acid as its *N*-9-fluorenylmethyloxycarbonyl derivative (Fmoc-AMPA-OH) in several steps, with an overall yield of 34%.

The assembly of peptide-ABA and peptide-APA (Scheme 1) differed from that of peptide-AMBA and peptide-AMPA (Scheme 2). In the synthesis of peptide-ABA and peptide-APA, the *O*-9-fluorenylmethyl esters of 4-aminobenzoic acid (H-ABA-OFm) and 4-aminophenylacetic acid (H-APA-OFm) were coupled to the γ-carboxylic acid of Boc-Glu-OBu^t in solution by the trimethylacetic acid (pivalic acid) mixed anhydride method. (Because of the poor nucleophilic character of the aniline moiety, use of the coupling reagents benzotriazolyloxy-tris-[dimethylamino] phosphonium hexafluorophosphate [BOP], O-benzotriazolyl-*N,N,N′,N′*-

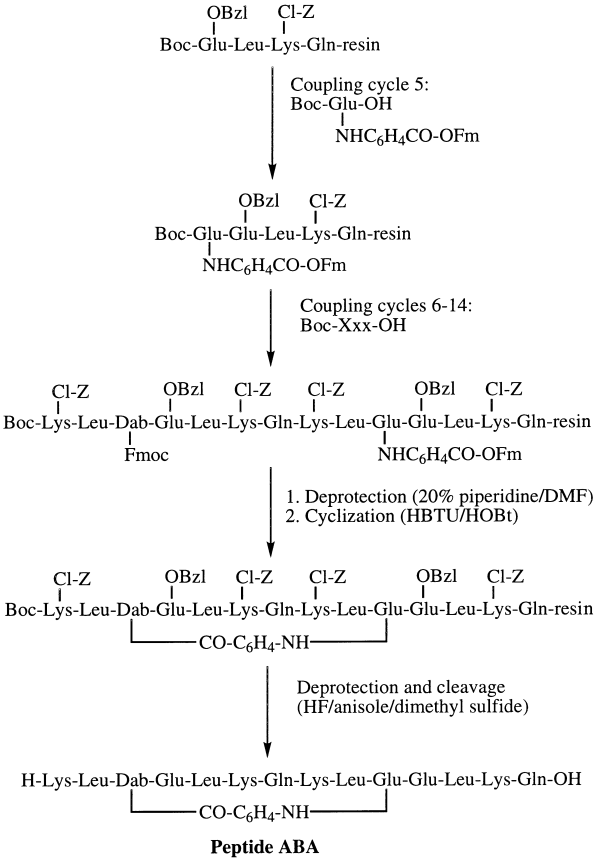

Scheme 1. Synthetic route to peptide ABA. The same procedure was used to synthesize peptide APA, except that Boc-Glu($NHC_6H_4CH_2CO$-OFm)-OH was used in coupling cycle 5, and Dab^3 was substituted by Dap.

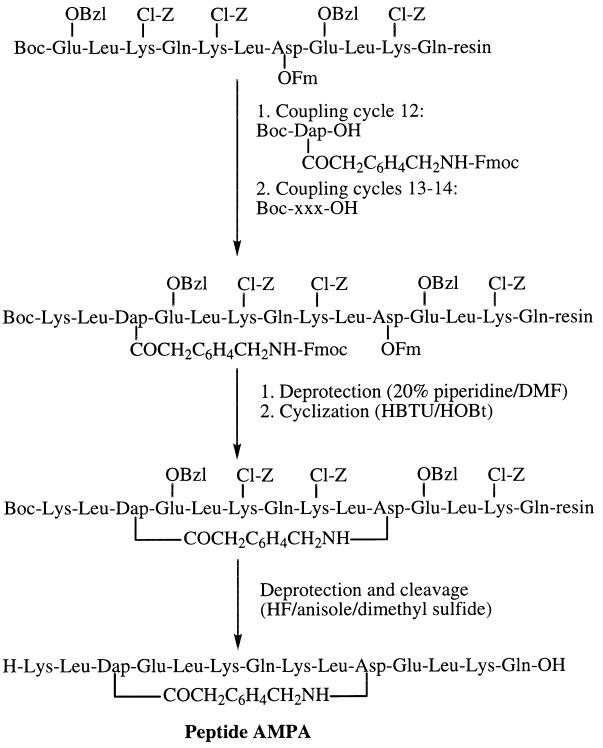

Scheme 2. Synthetic route to peptide AMPA. The same procedure was used to synthesize peptide AMBA, except that Boc-Dap($COC_6H_4CH_2NH$-Fmoc)-OH was used in coupling cycle 12, and Asp^{10} was substituted by Glu.

tetramethyluronium hexafluorophosphate [HBTU], or *N,N′*-dicyclohexylcarbodiimide [DCC] for this reaction resulted in very little product.) Acidolytic deprotection of the α-amine and α-carboxylic acid, followed by selective reprotection of the α amine, then afforded Boc-Glu(ABA-OFm)-OH and Boc-Glu(APA-OFm)-OH as the pseudodipeptide building blocks needed for the solid-phase assembly of these peptides. In the synthesis of peptide-AMPA and peptide-AMBA (Fig. 2), the corresponding pseudodipeptides, Boc-Dap(N-Fmoc-AMPA)-OH and Boc-Dab(N-Fmoc-AMBA)-OH, were prepared efficiently in solution in one step by the *N*-hydroxysuccinimide active ester (-OSu) method, without needing to protect the benzoic, phenylacetic acid group.

Peptide chains were assembled on Merrifield resin or hydroxymethylpolystyrene resin, using a moderate peptide substitution level (about 0.3 mequiv/g resin) in order to minimize interchain coupling during the cyclization reactions. Elongation of the peptide chains and side-chain to side-chain cyclizations were all performed using HBTU, HOBt, and DIEA in DMF and DCM (2/1). The final deprotection and cleavage from resin was carried out using HF/anisole/dimethyl sulfide (10/1/1). Despite reported side reactions[22] when HBTU is used in cyclization reactions (which we also have observed in other syntheses), the peptide chain assembly, cyclization and deprotection/cleavage steps in these syntheses were very successful, and crude peptides of high purity, as characterized by reversed-phase (RP) HPLC, were obtained. The crude peptides were each then purified to apparent homogeneity by RP-HPLC.

Circular dichroism spectra in aqueous solution

CD spectra of the four monocyclic, (i, i+7)-bridged model peptides described in Figure 2 were measured in aqueous 10 mM phosphate buffer, pH 7.0, at 25 °C. For comparison, the dicyclic, (Lys^i, Asp^{i+4})-bridged model peptide 2-2, and the linear analogue peptide 3-3 were also studied under the same conditions, as reported previously.[13] These spectra are all shown in Figure 3, with mean residue ellipticities, [θ] (deg cm^2 dmol^{-1}), calculated per residue using $n = 14$. The (i, i+7)-bridged model peptides gave CD spectra indicative of different mixtures of α-helical and disordered conformation. The CD spectrum of peptide AMPA was consistent with the highest α-helical content in this group, as indicated by the strong positive peak at around 190–192 nm, and the double negative peaks near 208 and 222 nm.[23,24] The value for [θ] measured for the α-helix n–π^* transition at 222 nm has been used to calculate an approximate fractional helix content, according to the equation:[23]

$$\% \text{ helix} = [\theta]_{222}/[\theta]_{max} \times 100\%,$$

$$\text{where } [\theta]_{max} = -39{,}500 \times (1 - [2.57/n])\text{deg}\cdot\text{cm}^2/\text{dmol}$$

By this estimation (Fig. 1 and Table 1), using $n = 14$ amino acid residues, the helix content of the monocyclic

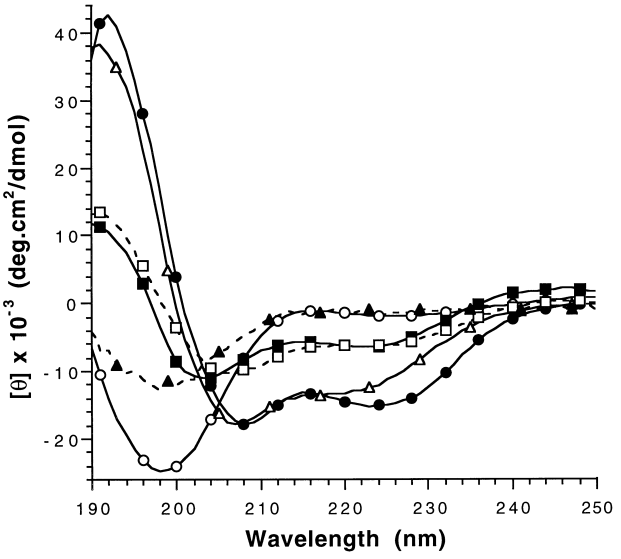

Figure 3. CD spectra of model peptides in aqueous 10 mM phosphate buffer, pH 7.0, at 25 °C: AMPA, 120 μM (●); AMBA, 118 μM (■); APA, 58 μM (□); ABA, 110 μM (o); 2-2, 57 μM, (△); 3-3, 57 μM (▲).

14-residue peptide AMPA at 25 °C is nearly 50%, compared to about 40% helix estimated for peptide 2-2. In contrast, peptide ABA gave a spectrum at 25 °C with a single, strong minimum at around 198 nm, and very little signal at 208 nm and 222 nm. This spectrum is indicative of mostly disordered structure with little or no α-helical or other ordered conformation present. The spectra of peptide AMBA and peptide-APA at 25 °C matched each other closely, and indicated a degree of helix stabilization by their bridges that is intermediate between that of the rigid 4-aminobenzoic acid bridge in peptide ABA and the more flexible unconjugated 4-(aminomethyl)phenylacetic acid bridge in peptide AMPA.

Quantitative linear regression analyses were performed to fit these peptide spectra to the standard spectra of Brahms and Brahms,[24] which are derived from polypeptide models (Table 2). Since the peptide concentrations had been accurately determined by amino acid analysis, the linear combinations were constrained to sum to 100% using the program LINCOMB.[25] This calculated fit gave results that were similar to those obtained by the single wavelength estimation, with 59%

Table 1 Helix contents of model peptides at 25 °C in aqueous phosphate buffer, pH 7.0. Estimated by the single wavelength method[a]

Peptide	In 100% aqueous buffer			In 50% TFE
	0 °C	25 °C	80 °C	25 °C
Peptide AMPA	51	47	35	62
Peptide APA	21	24	19	63
Peptide AMBA	13	20	21	58
Peptide ABA	0	5	15	29
Peptide 2-2[b]		41		64
Peptide 3-3[b]		12		40

[a]Fractional helix content, calculated according to the equation % helix = $[\theta]_{222}/[\theta]_{max} \times 100\%$, where $[\theta]_{max} = -39500 \times (1-[2.57/n])$ deg cm^2/dmol.
[b]Data taken from ref 13.

Table 2 Quantitative analysis of the CD spectra of peptides at 25 °C in aqueous phosphate buffer, pH 7.0[a]

Peptide	% Secondary structure in aqueous buffer		
	α Helix	β Sheet	Unordered
Peptide AMPA	59	16	25
Peptide APA	22	29	49
Peptide AMBA	18	32	50
Peptide ABA	3	18	79
Peptide 2-2	50	20	30

[a]Peptide spectra were fit to linear combinations of the standard spectra of Brahms and Brahms.[24]

α-helix determined for peptide-AMPA and 50% α-helix obtained for peptide-2-2. Next in helix content were peptide APA (22% α-helix) and peptide AMBA (18% α-helix). By this method, peptide ABA was less than 3% α-helical. As a further test of our conclusions, we performed quantitative linear regression analyses for the four model peptides to fit their spectra to the standard 5-component basis set described by Perczel et al.,[25] which is derived from the spectra of globular proteins of known three-dimensional structure. Although this protein-derived standard data set may be less appropriate for the analysis of peptide spectra, calculated values for α-helix content by this method were again very similar to those determined by the other methods: 47% for peptide-AMPA, 41% for peptide-2-2, 20% for peptide-AMBA, 24% for peptide-APA, 12% for peptide-3-3 and 5% for peptide-ABA. In addition, this method indicated that best fits were obtained when the spectral component attributed to aromatic and disulfide bridge contributions was zero (data not shown).

All of the above calculations assume that no contributions to the fitted far-UV CD spectra arise from the amide groups and benzene rings of the side-chain to side-chain lactam bridges. However, constrained aromatic structures in a chiral environment can sometimes give rise to strong CD spectra in the far UV region. Indeed, we noticed that peptide AMBA gave a small ellipticity signal at about $\lambda = 240$–250 nm ($+2000$ deg cm^2/dmol). This signal is attributed to the *p*-(aminomethyl)benzoic acid residue in the side-chain bridge, since the UV spectrum of peptide AMBA has an absorbance band at $\lambda_{max} = 237$. The UV spectra of the other three (i, i + 7)-bridged peptides also have absorption bands in this region, with $\lambda_{max} = 255$ nm for peptide APA, $\lambda_{max} = 270$ nm for peptide ABA, and only a very weak absorbance in this region for peptide AMPA. The contribution of these aromatic bridges to the CD signals used in our curve-fitting calculations (190 nm to 240 nm) is unknown.

The dependencies of the CD spectra on peptide concentration were also investigated in the same aqueous buffer at 25 °C, in order to determine whether or not the amphiphilic character of the model peptides in the α-helical conformation favored self-association and consequent helix stabilization. Within experimental error, there were no concentration-dependent changes in the CD spectra of peptide-AMPA, the most α-helical peptide,

in the concentration range between 2 μM and 240 μM. Similar results have been obtained previously[13] for the dicyclic peptide 2-2 over an even wider range (1 μM to 2 μM), indicating that neither peptide is changing its aggregation state in this concentration range. Concentration-dependent aggregation at lower concentrations than 2 μM is without precedent in peptides of this size and hydrophilic character, and considered very improbable. Therefore, we concluded that these peptides exist as monomers in aqueous solution (also see below).

CD melting curves

The temperature dependencies of the conformations of the model peptides were initially investigated by following $[\theta]_{222}$ as the temperature of the peptide solution was increased stepwise from 0 °C to 90 °C. The melting curves obtained for peptide AMPA and peptide-2-2 were gently sloping, nonsigmoidal (almost straight) denaturation curves, indicative of a gradual, noncooperative and incomplete heat denaturation process (Fig. 4). A set of complete spectra measured for peptide AMPA at 0, 25, 40, and 80 °C is also shown (Fig. 5). Again, the small temperature-dependent changes observed are consistent with a coil–helix equilibrium, and with only a partial denaturation of the helical structure in this peptide with increasing temperature. Indeed, the single wavelength estimation based on $[\theta]_{222}$ gives a value of 35% helix for peptide AMPA at 80 °C (Table 2). The melting curves of peptide AMBA , and peptide APA showed very little temperature dependency, and the negative ellipticity signal at 222 nm for peptide ABA even increased somewhat in magnitude with increasing temperature, as is typical for disordered peptides.[14,26] The CD spectra obtained for these peptides at 80 °C are shown together in Figure 6. These spectra are all similar to those obtained at 25 °C, and are likewise indicative of mixed disordered and helical structures, with no significant new spectral characteristic apparent at the higher temperature.

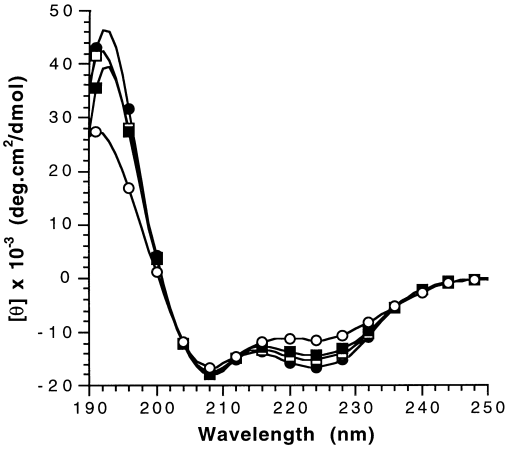

Figure 5. CD spectra of peptide AMPA at different temperatures. The CD spectrum of peptide AMPA (120 μM) in aqueous 10 mM phosphate buffer, pH 7.0, was measured at 0 °C (●), 25 °C (□), 40 °C (■), and 80 °C (o).

The annealing curves obtained by cooling peptide AMBA and peptide AMPA solutions from 90 to 0 °C were also measured, and were superimposable on the melting curves within experimental error (not shown), indicating that the small melting effects observed were completely reversible. To confirm that peptide AMPA is monomeric in aqueous solution, we measured its melting curve from 0 to 90 °C at different concentrations ranging from 2 to 240 μM (not shown). Concentration dependencies in the data were also small and within the experimental errors, further demonstrating that this peptide exists in the monomeric state in aqueous solution in this concentration range.

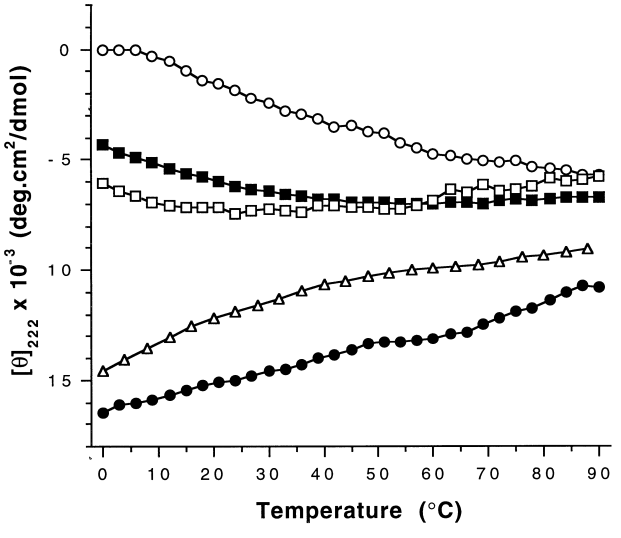

Figure 4. Thermal denaturation of model peptides followed by CD. Ellipticity at 222 nm was followed for solutions of 120 μM AMPA (●), 118 μM AMBA (■), 59 μM APA (□), 110 μM ABA (o), and 57 μM 2-2 (Δ), in 10 mM phosphate buffer, pH 7.0.

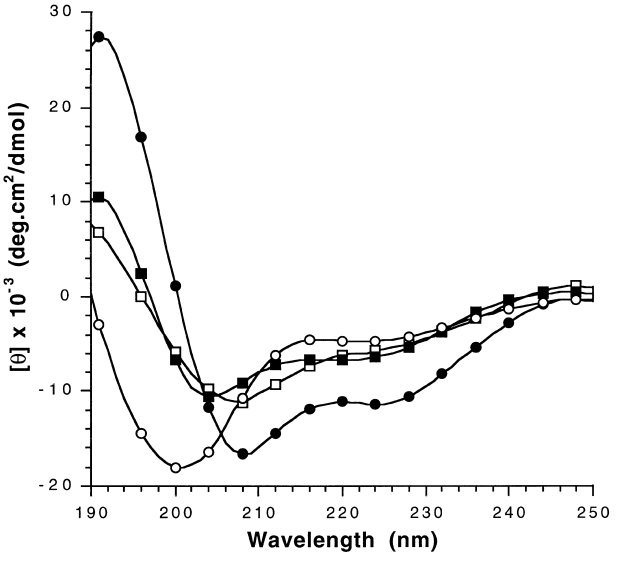

Figure 6. CD spectra of model peptides at 80 °C. Peptide spectra were measured in aqueous 10 mM phosphate buffer, pH 7.0, at 80 °C: AMPA, 120 μM (●); AMBA, 118 μM (■); APA, 58 μM (□); ABA, 110 μM (o).

CD spectra in 50% (v/v) trifluoroethanol

From Figure 1, it can be seen that the introduction of an additional helix stabilizing factor is necessary to distinguish the relative stabilities of the α-helical conformations of predominantly unordered peptides, such as peptide ABA and peptide 3-3, from their CD spectra. Therefore, the effects of the helix-promoting solvent 2,2,2-trifluoroethanol (TFE)[26] on the CD spectra of the monocyclic (i, i + 7)-bridged model peptides were investigated. Addition of TFE to a level of 50% (v/v), where the helix stabilizing effects of this solvent are known to be maximal,[26] enhanced the α-helix contents of all four of the (i, i + 7)-bridged model peptides at 25 °C, as indicated by the stronger minima in their CD spectra at around 208 nm and 222 nm (Fig. 7).

The greatest changes in the CD spectra due to addition of the TFE were observed for peptide APA and AMBA, although peptide AMPA remained the most helical peptide. Quantitative analysis of these spectra for peptide secondary structure composition using the standard spectra of Brahms and Brahms[24] indicated that peptides APA and AMBA were about 60% helical in this solvent mixture, compared to about 75% helix calculated for peptide AMPA (Table 3). This suggests that the i, i + 7 side-chain bridges in peptide APA and peptide AMBA are compatible with the α-helical conformation, but somewhat less effective for helix stabilization compared to the bridge in peptide AMPA. In 50% (v/v) TFE, peptide ABA was clearly the least helical of the model (i, i + 7)-bridged peptides studied here (Table 3). Indeed, a comparison of its mean residue ellipticity at 222 nm with that of peptide 3-3 (Table 1) indicates that it has a lower helix forming propensity than even the linear analogue with this amino acid sequence, suggesting that the 4-aminobenzoic acid-based i, i + 7 side-chain link is, in fact, helix destabilizing or favors an alternative conformation.

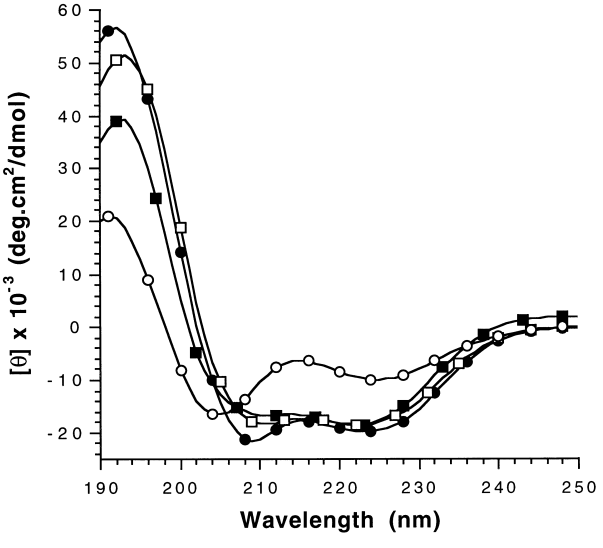

Figure 7. CD spectra of peptides in 50% (v/v) TFE. The CD spectra were recorded in 1:1 (v/v) mixture of TFE and 20 mM phosphate buffer, pH (1/1, v/v): AMPA, 120 μM (●); AMBA, 118 μM (■); APA, 58 μM (□); ABA, 110 μM (○).

Table 3 Quantitative analysis of the CD spectra of model peptides in 50% (v/v)[a]

Peptide	% Secondary structure in 50% TFE		
	α Helix	β Sheet	Unordered
Peptide AMPA	75	16	9
Peptide APA	60	34	6
Peptide AMBA	58	19	23
Peptide ABA	37	16	47

[a]Trifluoroethanol at 25 °C in aqueous phosphate buffer, pH 7.0. Peptide spectra were fit to linear combinations of the standard spectra of Brahms and Brahms.[24]

Analysis of helix stabilization by RP-HPLC

In peptides with the potential to form amphiphilic α-helical structure, correlations between enhanced helix stability and increased retention time on RP-HPLC columns have long been observed.[27–29] This correlation is assumed to be the result of hydrophobic binding by the lipophilic face of the amphiphilic helix with the lipophilic stationary phase of the column being a predominant factor determining peptide retention time on the column. If differences in the strength of this mode of binding, which is dependent on the stability of the α-helical conformation, outweigh differences in the direct hydrophobic interactions of individual structural components in a series of peptides, then the correlation will hold.

Because of the unknown potential for the side-chain bridges to interfere with the quantification of relative α-helix contents in our model peptides, there remained some doubt about their relative helix forming propensities. We were, therefore, interested in confirming the relative helix stabilities of these model peptides using the RP-HPLC method. This series of model (i, i + 7)-bridged peptides provides an ideal system to study by this method: the hydrophobic face that is formed by these peptides in the α-helical conformation is unaltered in the series, and the bridges on the hydrophilic face in this peptide series are structurally similar constitutional isomers, and should, therefore, have essentially identical, direct, localized hydrophobic interactions with the column by themselves.

All four (i, i + 7)-bridged peptides were eluted together on an analytical C_{18} reversed-phase column, using an acetonitrile gradient in aqueous 0.1% (v/v) trifluoroacetic acid (TFA) buffer, pH 2.1. The elution profile, which was determined by monitoring UV absorbance at 220 nm, is shown in Figure 8. The identities of the individual peptide peaks were each confirmed by separate individual elutions. The most α-helical peptide under all of the conditions analyzed by CD, peptide AMPA, also had the longest retention time in this RP-HPLC chromatograph. The least α-helical peptide in the CD studies, peptide ABA, had the shortest retention time, eluting much earlier than the other three peptides in this series. The retention times of peptides APA and AMBA were intermediate between these extremes, again corresponding to the closely matching

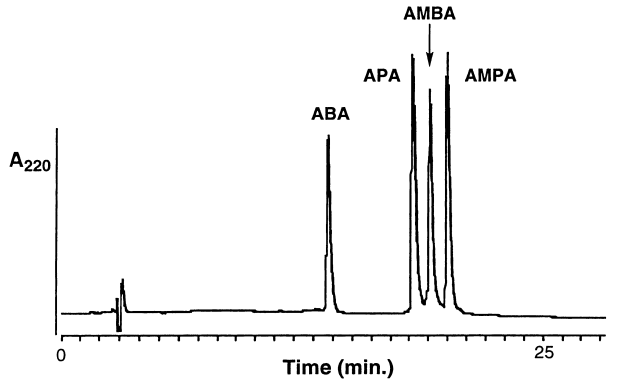

Figure 8. RP-HPLC of mixed peptides to determine relative retention times. The HPLC-pure peptides were mixed in approximately equimolar quantities and then the mixture was eluted from a C_{18} analytical RP-HPLC column. Peptides were eluted in the order: peptide ABA, peptide APA, peptide AMBA and then peptide AMPA (from left to right), using a gradient of 10–40% buffer B in buffer A from 0 to 25 min after the sample injection, and a flow rate of 1.2 mL/min. Buffer A consisted of 10% (v/v) acetonitrile and 0.1% (v/v) TFA in H_2O; buffer B consisted of 90% (v/v) acetonitrile and 0.1% (v/v) TFA in H_2O. The eluate was monitored by measuring UV absorbance at 220 nm.

intermediate helix contents determined for these peptides from the CD experiments (Tables 1–3). However, peptide APA eluted slightly earlier than peptide-AMBA, although its helix content was determined from its CD spectra to be slightly higher than that of peptide AMBA. Overall, therefore, the RP-HPLC retention times agreed with the CD analyses well, despite being performed at much lower pH: peptide AMPA was assessed as the most helical peptide by this method, and the particularly short retention time of peptide ABA indicated that it had a much lower helix-forming propensity than the other three (i, i + 7)-bridged peptides.

Discussion

The synthesis of the four monocyclic, (i, i + 7)-bridged peptides reported here (Fig. 2), which are based on the 7-residue repeating model amphiphilic α-helical peptide sequence used previously to study (i, i + 4)-lactam bridged peptides, was successfully accomplished in good yield by synthetic methods based on those of Felix and co-workers.[5] In each case, the solid-phase cyclizations were complete in only a few hours, and little polymeric byproduct was observed by analytical RP-HPLC. Therefore, at least in this peptide sequence context, the 35-atom ring macrocyclizations required to incorporate these rigid side-chain bridges into a peptide structure were found to be remarkably favorable reactions, although similar solid-phase cyclizations involving smaller rings can often give poor yields.[30]

In aqueous solution at temperatures ranging from 0 to 90 °C, and in mixed aqueous and organic solvent (50% TFE) at 25 °C, qualitative and quantitative analyses of the CD spectra of these (i, i + 7)-bridged peptides at pH 7.0 all indicate different mixtures of predominantly α-helical and unordered (coil) structure. Consistently, the α-helix contents of these model peptides follow the order peptide AMPA > peptide APA = peptide AMBA > peptide ABA. This order indicates a clear correlation between α-helix stabilization by these bridges, which are constitutionally isomeric structures, and the positions of the two amide linkages within the bridge. The AMPA bridge has methylene groups inserted between both amides and the central benzene ring, whereas both the APA and the AMBA bridges have one amide bond directly linked to, and in conjugation with, the benzene ring. The ABA bridge has a fully conjugated bridging π-electron system, in which both amide bonds are linked directly to the central benzene ring. This suggests that these bridges may not all exactly match the requirements of the (i, i + 7)-side-chain linkage on the surface of an α-helix, and that increased flexibility in the bridges going from the ABA bridge to the AMPA bridge may allow a better conformational adaptation of the bridge to the α-helical structure.

Assessing the energetic value of the helix stabilizing effects of the optimal Dap(AMPA)^{i}, Asp^{i+7} bridge is complicated by the fact that peptide AMPA does not show cooperative melting behavior in aqueous solution (Fig. 4), and that its UV-absorbing side-chain bridge may interfere with the CD spectra obtained. The conclusion that peptide AMPA is substantially helical in solution is supported by the agreement between our analyses of the CD spectra for α-helix content (Tables 1–3) and the RP-HPLC elution profile for the peptides shown in Figure 8, since increased retention times on RP-HPLC columns are observed to correlate with increased helix stability for amphiphilic α-helical peptides.[27–29] In addition, the melting behaviors of these four peptides, as well as the effect of 50% TFE and the quantitative curve-fitting analyses of their CD spectra, are all consistent with expectations for coil–helix equilibria based on standard peptide spectra, without indicating the presence of any extra spectral component due to the side-chain bridges. Therefore, if the side-chain bridges do contribute to the CD spectra, this contribution appears to be small.

Comparing the monocyclic (i, i + 7)-bridged peptides in this study with the related model peptides, dicyclic peptide 2-2 and linear peptide 3-3, demonstrates that the single Dap(AMPA)^{i}, Asp^{i+7} bridge in peptide AMPA is approximately as effective for helix stabilization in aqueous solution as the two Lys^{i}, Asp^{i+4} bridges in peptide 2-2 (Tables 1 and 2, and Fig. 3). In contrast, the Dab^{i}(ABA), Glu^{i+7} bridge in peptide ABA appeared to be helix destabilizing (i.e., it favors an alternative, non-helical conformation), when compared to the linear peptide 3-3 (Table 3). This, in turn, suggests that the i, i + 7 bridge in peptide AMPA may be worth about 1 kcal/mol of helix stabilization free energy, by comparison to the effects of the i, i + 4 bridges reported elsewhere.[9,10] Its effectiveness cannot easily be compared to the other i, i + 7 side-chain bridges reported in the literature to date,[18,20] because of differences in the underlying peptide sequence contexts of these bridges, and the use of helix stabilizing end-capping N^{α}-acetyl

and C^{α}-amide groups in these other systems, although all of the reported (i, i+7)-bridged systems have similar lengths (13–16 residues). Jackson et al. reported[18] values of $[\theta]_{195}$ and $[\theta]_{222}$ near +25,000 and −30,000 deg cm^2/dmol, respectively, at 0 °C in 0.1% aqueous TFA solution for their D-thiolysine,[4] L-thiolysine[11] disulfide-bridged peptide 5. Phelan et al. reported[20] similar CD spectral intensities at 7 °C in aqueous solution at pH 5 for their peptide **1c**, which has the side chains of Glu^3 and Glu^{10} linked by amide bonds to 1,3-diaminopropane. In comparison, peptide AMPA gave a $[\theta]_{222}$ value of only −16,400 deg cm^2/dmol at 0 °C in neutral aqueous buffer, but had a stronger maximum at lower wavelength ($[\theta]_{195}$ = +38,000 deg cm^2/dmol). This matched the corresponding spectrum of the dicyclic (i, i+4)-bridged peptide 2-2 more closely (Fig. 3). Based on the CD signals at 222 nm, therefore, peptide AMPA appears to be somewhat less helical than these other monocyclic, (i, i+7)-bridge peptides, but it is somewhat more helical if the comparison is based on the ellipticity maximum at 190 nm. The overall shapes of these spectra are, therefore, somewhat different, and this may invalidate comparisons based on ellipticities at any single wavelength.

Interestingly, a comparison of the melting behaviors of all three of the (i, i+7)-bridged peptide systems reported to date (peptide AMPA here, peptide 5 in ref 18, and peptide **1c** in ref 20) shows that the helical structure in peptide AMPA is the most resistant to thermal denaturation, perhaps as a result of the relative rigidity of its side-chain bridge structure. This is most easily seen by comparing the loss of ellipticity with increasing temperature near the maximum for α-helix at 190 nm, although the difference is also seen at 222 nm: at 80 °C, $[\theta]_{195}$ for peptide AMPA was still strongly positive, having a value of +20,300 deg cm^2/dmol. In contrast, peptide 5 of Jackson et al.[18] and peptide **1c** of Phelan et al.[20] were both reported to have negative $[\theta]_{195}$ values at this temperature, indicating that the negative ellipticity peak near 197 nm that is characteristic of unordered structure had become dominant. The $Dap(AMPA)^i$, Asp^{i+7} bridge may, therefore, be advantageous for helix stabilization for peptides acting in vivo at 37 °C.

Conclusion

Four isomeric, rigid, side-chain to side-chain bridges that use amide bonds on *para*-substituted benzene rings to link the 3rd and the 10th residues in a model 14-residue peptide have been designed for α-helix stabilization (Fig. 2). These monocyclic peptides were successfully synthesized in good yield, by standard solid-phase methods,[5] using orthogonal protecting groups for the side-chain functionalities involved in the macrocyclization reaction during peptide elongation. Analysis of the conformational properties of these peptides in solution by CD, and their retention times on RP-HPLC columns, indicates that the most successful bridge design is the $Dap(AMPA)^3$, Asp^1 bridge in peptide AMPA, and that this bridge is approximately as effective for helix stabilization as the two Lys^i, Asp^{i+4} side-chain bridges in peptide 2-2 (Fig. 2). In comparison to other i, i+7 bridges reported in the literature,[18,20] this bridge appears to produce a helical structure that is more resistant to heat denaturation (Fig. 4). Further investigation is required, in order to determine whether or not the helical structure the AMPA bridge stabilizes has a regular α-helical conformation, and exactly how much stabilization energy it contributes. Nevertheless, this new i, i+7 bridge design offers an alternative, synthetically accessible approach to helix constraint and stabilization that is generally applicable to structure–activity studies of bioactive α-helical peptide ligands.

Experimental

Materials and methods

Protected L-amino acids were purchased from Bachem Bioscience, NovaBiochem, or Advanced ChemTech, and used without further purification. Merrifield resin and hydroxylmethyl resin (1% cross-linked, 100–200 mesh) were purchased from Advanced ChemTech. Dichloromethane (DCM), *N*,*N*-dimethylformamide (DMF), 2-propanol, (*i*-PrOH), methanol (MeOH), and acetonitrile were HPLC grade or equivalent and were purchased from Fischer Scientific or Aldrich and used without further purification. *N*,*N*′-diisopropylethylamine (DIEA, Aldrich) was dried over KOH and distilled over ninhydrin. Trifluoroacetic acid (TFA) was purchased from Halocarbon. BOP, HBTU, 1-hydroxylbenzotriazole (HOBt) and DCC were purchased from NovaBiochem and Advanced ChemTech. Lithium aluminum hydride, 4-(aminomethyl)benzoic acid, 4-aminobenzoic acid, 4-aminophenylacetic acid, trimethylacetyl chloride, pyridine, piperidine, acetic anhydride and 2,2,2-trifluoroethanol (TFE) were purchased from Aldrich. All other peptide synthesis reagents were purchased from Advanced ChemTech.

Prior to amino acid analysis, peptides were hydrolyzed in 6 N HCl (Pierce) at 110 °C for 24 h. Amino acid analyses was performed in the laboratory of Dr. Stanley Stein, Center for Biotechnology and Medicine, Rutgers University, Piscataway, New Jersey. Mass spectrometry was performed using either matrix-assisted laser desorption ionization or electrospray ionization, at the Protein and Carbohydrate Analysis Facility, University of Michigan, Ann Arbor, Michigan. NMR spectra were recorded at 200 MHz. Element analyses were performed by Quantitative Technologies Inc., Whitehouse, New Jersey. Reverse-phase high-pressure liquid chromatography (RP-HPLC) was performed on dual-pump Rainin or Perkin Elmer HPLC systems. Peptides were eluted on C_{18} Dynamax-300A columns with a 5 μM particle size (4.6 mm×25 cm for analytical separation, and 10 mm×25 cm for preparative separations). Flow rates were 1.2 mL/min and 3.0 mL/min for the analytical and preparative separations, respectively. Eluting buffers were as follows: buffer A, 0.1% (v/v) TFA in 10% CH_3CN/water; buffer B, 0.1% (v/v) TFA in 90% CH_3CN/water. Elution was monitored by UV absorbance at 220 nm.

N-Fmoc-4-(Aminomethyl)benzoic acid.[31] 4-(Aminomethyl)benzoic acid (3.33 g, 22.0 mmol) was dissolved in 5% (w/v) $NaHCO_3$ aqueous solution (100 mL). A solution of *N*-(9-fluorenylmethyloxycarbonyl)oxysuccinimide[41] (Fmoc-OSu) (6.75 g, 20.0 mmol) in dioxane (100 mL) was then added. The mixture was stirred for 2 h at room temperature (rt). Then 10% (w/v) citric acid (50 mL) was added and the solvents were evaporated in vacuo at 30 °C. The solid was washed with water and then dissolved in dioxane and dried over Na_2SO_4 overnight. The dioxane was evaporated and the crude product was recrystallized from dioxane and hexane: Yield 5.8 g (77.7%); mp 226–228 °C; ^{1}H NMR (DMSO-d_6) δ 7.8–7.9 (m, 5H), 7.6–7.7 (d, 2H), 7.2–7.5 (m, 6H), 4.3–4.4 (d, 2H), 4.2–4.25 (m, 3H).

N^{α}-*t*-Boc-(L)-2,4-diaminobutyric acid (Boc-Dab-OH).[32–34] Boc-(L)-Gln-OH (4.98 g, 20 mmol) was dissolved in 100 mL of a mixture of acetonitrile/water (2/1, v/v). Bis(trifluoroacetoxy)-phenyliodine (12.6 g, 40 mmol) and DIEA (5.16 g, 40 mmol) was added. The reaction solution was stirred overnight at rt. The solvents were then evaporated and water (100 mL) was added. The resultant suspension was extracted with diethyl ether (3×100 mL). The clear aqueous solution was then evaporated. Chloroform (30 mL) was added into the oily residue and crystalline material formed. The crude product was recrystallized from methanol and ether and dried in vacuo: Yield 3.12 g (70.6%); mp 212–214 °C (lit.[34] for D-enantiomer, 197–198 °C); ^{1}H NMR (CD_3OD) δ 4.6 (br, 1H), 3.9–4.0 (m, 1H), 3.0 (t, 2H), 2.0–2.1 (m, 1H), 1.9–2.0 (m, 1H), 1.45 (s, 9H); Elemental analysis calcd for $C_9H_{18}N_2O_4 \cdot 1/2\ H_2O$): C, 47.56; H, 8.43; N, 12.33. Found: C, 47.51; H, 8.45; N, 12.31.

N^{α}-*t*-Boc-N^{γ}-(*N*-Fmoc-4-aminomethylbenzoyl)-(L)-2,4-diaminobutyric acid (Boc-Dab[Fmoc-AMBA]-OH). *N*-Fmoc-4-(aminomethyl)benzoic acid (4.11 g, 11 mmol) was dissolved in 200 mL of dioxane and ethyl acetate (2/1, v/v). *N*-hydroxysuccinimide (1.31 g, 11.0 mmol) and DCC (2.50 g, 12.1 mmol) was added and the mixture was stirred for 20 h at rt. The DCU was then removed by filtration and washed with a mixture of ethyl acetate and dioxane (1/1). The solvents were evaporated. The residue was then dissolved in 100 mL of dioxane. A solution of Boc-(L)-Dab-OH (2.62 g, 12 mmol) in water (50 mL) and DIEA (1.94 g, 15.0 mmol) were added. The reaction mixture was stirred overnight at rt. Then 10% (w/v) citric acid (50 mL) was added and most of the dioxane was removed by evaporation. The aqueous mixture was extracted with ethyl acetate (3×200 mL). The organic layer was washed with 10% citric acid and water, dried over Na_2SO_4, and evaporated. The solid was recrystallized from ethanol and ether: Yield 3.86 g (67.3%); mp sublimes at 107 °C; ^{1}H NMR (DMSO-d_6) δ 12.25 (br, 1H), 8.23 (br, 1H), 7.70–7.95 (m, 7H), 7.28–7.50 (m, 6H), 7.20 (d, 1H), 4.39 (d, 2H), 4.24 (m, 3H), 3.95–4.05 (m, 1H), 3.3 (m, 2H), 1.95–2.05 (m, 1H), 1.75–1.85 (m, 1H), 1.41 (s, 9H); Elemental analysis calcd for $C_{32}H_{35}O_7N_3$: C, 67.00; H, 6.15; N, 7.33. Found: C, 66.79; H, 6.27; N, 7.20.

N^{α}-*t*-Boc-N^{γ}-Fmoc-(L)-2,4-diaminobutyric acid (Boc-Dab[Fmoc]-OH).[34] Boc-Dab-OH (2.40 g, 11 mmol) was dissolved in 50 mL of 5% (w/v) $NaHCO_3$. Fmoc-OSu (3.37 g, 10 mmol) in 50 mL of dioxane was added into this solution. The mixture was stirred for 2 h at rt and then extracted with diethyl ether. The aqueous layer was acidified with 10% (w/v) citric acid and extracted with DCM. The organic layer was washed with water, dried over Na_2SO_4, evaporated, and then recrystallized from chloroform and hexanes: Yield 3.5 g (79.5%); mp sublimes at 90 °C (lit. sublimes at 85–95 °C); ^{1}H NMR ($CDCl_3$) δ 7.76 (d, 2H), 7.60 (d, 2H), 7.30–7.45 (m, 4H), 5.50–5.60 (br, 1H), 5.30–5.40 (br, 1H), 4.40 (m, 3H), 4.20–4.30 (m, 1H), 3.10–3.25 (br, 2H), 1.8–2.0 (br, 2H), 1.46 (s, 9H); Elemental analysis calcd for $C_{24}H_{28}N_2O_6$: C, 65.44; H, 6.41; N, 6.36. Found, C, 65.33; H, 6.45; N, 6.27.

***O*-9-Fluorenylmethyl-*N*-Boc-4-aminobenzoate.** (*N*-Boc-ABA-OFm). 4-Aminobenzoic acid (13.71 g, 100 mmol) and triethylamine (TEA) (10.12 g, 100 mmol) was dissolved in 250 mL of dioxane and water (3/1). Then di-*t*-butylpyrocarbonate (24.0 g, 110 mmol) was added.[40] The mixture was stirred for 3 days at rt. Most of solvent was removed by evaporation, then 200 mL of 10% (w/v) citric acid was added. The mixture was extracted with ethyl acetate (3×300 mL). The organic layer was washed with 10% (w/v) citric acid and water, dried over $MgSO_4$, and then evaporated to dryness. The residue was precipitated from ethyl acetate and hexanes: Yield 14.5 g (61.2%); ^{1}H NMR (CD_3OD) δ 7.95 (d, 2H), 7.50 (d, 2H), 1.53 (s, 9H).

The *N*-Boc-4-aminobenzoic acid (11.9 g, 50 mmol) was then dissolved in 300 mL of dioxane and DCM (1/1, v/v). 9-Fluorenemethanol (9.8 g, 50 mmol), DCC (11.3 g, 55 mmol), and 4,4-dimethylaminopyridine (DMAP) (122 mg, 1 mmol) were added. The mixture was stirred for 3 days at rt. DCU was then removed by filtration and the solvents were evaporated. The residue was dissolved in DCM. This solution was washed with 2.5% (w/v) $NaHCO_3$, 5% (w/v) citric acid, and then water, dried over Na_2SO_4, and precipitated from ethyl acetate and hexanes: Yield 12.5 g (62%); ^{1}H NMR ($CDCl_3$) δ 9.0 (s, 1H) 8.1 (d, 2H), 7.6–8.0 (m, 6H), 7.3–7.5 (m, 4H), 4.58 (d, 2H), δ 4.4 (t, 1H), 1.47 (s, 9H).

N^{α}-*t*-Boc-(L)-Glu(ABA-OFm)-OtBu.[35] *O*-9-Fluorenylmethyl-*N*-*t*-Boc-4-aminobenzoate (*N*-Boc-ABA-OFm) (8.67 g, 20 mmol) was dissolved in 100 mL of TFA. The solution was stirred for 1 h at rt. Then the TFA was evaporated. DCM (100 mL) was added and then evaporated again three times, to remove residual TFA. The residue was then dried under vacuum.

Boc-(L)-Glutamic acid-α-*t*-butyl ester (Boc-Glu-OBu^t) (6.06 g, 20 mmol) was dissolved in 100 mL of anhydrous benzene. DIEA (2.59 g, 20 mmol) was added and the solution was cooled to −5 °C. Trimethylacetyl chloride (2.42 g, 20 mmol) was added. The solution was stirred for 2 h at 0 °C and for 2 h at rt. Then another 5.83 g (45 mmol) of DIEA was added. The solution of the TFA salt of 4-aminobenzoic acid-9-fluorenylmethyl

ester in 200 mL of anhydrous dioxane and benzene (1/1) was added into the mixed anhydride mixture. The reaction solution was stirred for 3 days at rt and for 4 h at 50 °C. The mixture was then evaporated, and the residue was dissolved in ethyl acetate. This solution was washed with 5% (w/v) $NaHCO_3$, water, 5% (w/v) citric acid, and water, then dried over Na_2SO_4, and evaporated. The residue was recrystallized from chloroform and hexanes, two times: Yield 7.1 g (59%); mp 115–117 °C; ^{1}H NMR ($CDCl_3$) δ 9.4 (br, 1H), 8.10 (d, 2H), 7.72–7.85 (m, 4H), 7.65 (d, 2H), 7.30–7.50 (m, 4H), 5.35–5.45 (m, 1H), 4.60 (d, 2H), 4.40 (t, 1H), 4.1–4.3 (m, 1H), 2.4–2.6 (m, 2H), 2.2–2.4 (m, 1H), 1.8–2.0 (m, 1H), 1.50 (s, 9H), 1.47 (s, 9H); Elemental analysis calcd for $C_{35}H_{40}O_7N_2$: C, 69.98; H, 6.71; N, 4.66. Found: C, 69.44; H, 6.82; N, 5.04.

N^{α}-Boc-(L)-Glu(ABA-OFm)-OH. N^{α}-Boc-(L)-Glu(ABA-OFm)-OBu^t (6.0 g, 10.0 mmol) was dissolved in 100 mL of TFA. The solution was stirred for 1 h at rt. The TFA was then removed by evaporation. DCM (100 mL) was added and evaporated again. The residue was dried under vacuum. Di-*t*-butyl dicarbonate (3.27 g, 15 mmol) and DIEA (3.87 g, 30 mmol) was dissolved in 100 mL of dioxane. The solution of the TFA salt of H-Glu(ABA-OFm)-OH (10 mmol) in 200 mL of dioxane and water (2/1) was added, dropwise, over 3 h at rt. The solution was stirred for another hour at rt, then neutralized by 10% (w/v) citric acid. Most of dioxane was evaporated. 5% (w/v) citric acid (200 mL) was added, and the mixture was extracted with ethyl acetate (3×200 mL). The organic layer was washed with 5% (w/v) citric acid and water, dried over Na_2SO_4, and then evaporated. The residue was precipitated from ethyl acetate and hexanes two times. The crude product was then purified by silica gel flash chromatography (eluent: $CHCl_3$/MeOH/AcOH, 20/1/1): Yield 3.5 g (64.3%); mp sublimes at 90 °C; ^{1}H NMR ($CDCl_3$) δ 8.90–8.95 (br, 1H), 8.04 (d, 2H), 7.6–7.8 (m, 6H), 7.30–7.42 (m, 4H), 5.60 (d, 1H), 4.58 (d, 2H), 4.30–4.50 (m, 2H), 2.50–2.65 (br, 2H), 2.28–2.45 (m, 1H), 2.0–2.2 (m, 1H), 1.47 (s, 9H); Elemental analysis calcd for $C_{31}H_{32}O_7N_2 \cdot H_2O$: C, 66.18; H, 6.09; N, 4.98. Found: C, 66.24; H, 6.03; N, 4.75.

N^{α}-*t*-Boc-(L)-2,3-diaminopropionic acid (Boc-Dap-OH).[32–34] Boc-Dap-OH was prepared from N^{α}-Boc-(L)-Asn-OH by the same procedure as that for Boc-Dab-OH: Yield 76.5%; mp 203–205 °C (lit. 198–200 °C dec;[33] 205–205.5 °C[34]); ^{1}H NMR (CD_3OD) δ 4.06 (t, 1H), 3.10–3.20 (two d, 2H), 1.47 (s, 9H); Elemental analysis calcd for $C_8H_{16}N_2O_4 \cdot 1/2\ H_2O$): C, 45.06; H, 8.04; N, 13.14. Found: C, 45.11; H, 8.07; N, 13.02.

N^{α}-*t*-Boc-N^{β}-Fmoc-(L)-2,3-diaminopropionic acid (Boc-Dap[Fmoc]-OH).[34] Boc-Dap(Fmoc)-OH was prepared from Boc-Dap-OH by same procedure as that for Boc-Dab(Fmoc)-OH: Yield 71.2%; mp sublimes at above 85 °C (lit. sublimes at 75–100 °C[34]); ^{1}H NMR (CD_3OD) δ 7.79 (d, 2H), 7.65 (d, 2H), 7.27–7.45 (m, 4H), 4.15–4.35 (m, 4H), 3.35–3.70 (m, 2H), 1.42 (s, 9H); Elemental analysis calcd for $C_{23}H_{26}O_6N_2$: C, 64.78; H, 6.15; N, 6.57. Found: C, 64.35; H, 6.09; N, 6.72.

9-Fluorenylmethyl-*N*-Boc-4-aminophenylacetate (Boc-APA-OFm). *N*-Boc-4-aminophenylacetic acid (Boc-APA-OH) was prepared by same procedure as that for Boc-ABA-OH. Boc-APA-OH (7.58 g, 30 mmol) was then dissolved in 300 mL of dioxane and DCM (1/1). 9-Fluorenemethanol (5.89 g, 30 mmol), DCC (6.80 g, 33 mmol), and DMAP (37 mg, 0.3 mmol) were then added. The mixture was stirred for 10 h at rt. The DCU was removed by filtration, and then the solvents were evaporated. The residue was dissolved in DCM and washed with 5% (w/v) $NaHCO_3$, water, 5% (w/v) citric acid, and water, then dried over $MgSO_4$ and evaporated. The residue was recrystallized from chloroform and hexanes: Yield 10.1 g (78.1%); mp 134–136 °C; ^{1}H NMR (DMSO-d_6) δ 9.32 (s, 1H), 7.87 (d, 2H), 7.20–7.52 (m, 8H), 7.06 (d, 2H), 4.35 (d, 2H), 4.20 (t, 1H), 3.60 (s, 2H), 1.47 (s, 9H).

N^{α}-*t*-Boc-(L)-Glu(APA-OFm)-OBu^t. *O*-9-Fluorenylmethyl-*N*-Boc-4-aminophenylacetate (8.59 g, 20 mmol) was dissolved in 100 mL of TFA. The solution was stirred for 1 h at rt. The TFA was evaporated. DCM (200 mL) was added and evaporated again. The residue was then dried under vacuum. Boc-(L)-Glu-O^{t}Bu (6.07 g, 20 mmol) and DIEA (2.60 g, 20 mmol) were dissolved in 100 mL of anhydrous benzene. The solution was cooled to −5 °C. Trimethylacetyl chloride (2.40 g, 20 mmol) was added. This solution was stirred for 2 h at 0 °C and 2 h at rt. The TFA salt of *O*-9-fluorenylmethyl-4-aminophenylacetate (20 mmol) was dissolved in 200 mL of anhydrous dioxane and benzene (2/1). DIEA (5.83 g, 45 mmol) was added, and then the above mixed anhydride solution was filtered into the solution of *O*-9-fluorenylmethyl-4-aminophenylacetate. This mixture was stirred for 3 days at rt and 2 h at 50 °C. The solvents were evaporated. The oil residue was dissolved in ethyl acetate and washed with 5% (w/v) $NaHCO_3$, water, 5% (w/v) citric acid, and then water, dried over Na_2SO_4, and evaporated. The residue was recrystallized from ethyl acetate and hexanes: Yield 9.3 g (75.6%); mp 77–80 °C; ^{1}H NMR ($CDCl_3$) δ 8.95 (s, 1H), 7.75 (d, 2H), 7.60 (d, 2H), 7.35–7.50 (m, 4H), 7.15–7.30 (m, 4H), 5.40 (d, 1H), 4.40 (d, 2H), 4.15–4.32 (m, 2H), 3.65 (s, 2H), 2.45 (t, 2H), 2.20–2.35 (m, 1H), 1.80–1.95 (m, 1H), 1.48 (s, 9H), 1.46 (s, 9H).

N^{α}-*t*-Boc-(L)-Glu(APA-OFm)-OH. N^{α}-*t*-Boc-(L)-Glu-(APA-OFm)-O^{t}But (7.4 g, 12.0 mmol) was dissolved in 100 mL of TFA. The solution was stirred for 30 min at rt. The TFA was evaporated, then 20 mL of 4 N HCl in dioxane was added. The precipitate was washed with diethyl ether. The solid was dissolved in 150 mL of dioxane and water (2/1). Di-*t*-butyl dicarbonate (3.3 g, 15 mmol) and DIEA (3.88 g, 30 mmol) were added, and the solution was stirred for 2 h at rt. The solvents were evaporated. The residue was dissolved in ethyl acetate. The solution was washed with 5% (w/v) citric acid and water, dried over $MgSO_4$ and evaporated. The solid was recrystallized from ethyl acetate and hexanes. The product was further purified by silica gel flash chromatography (eluent: $CHCl_3$/MeOH/AcOH, 20/1/1): Yield 4.1 g (61.2%); mp sublimes at above 88 °C; ^{1}H NMR ($CDCl_3$) δ 8.62 (s, 1H), 7.74 (d, 2H), 7.32–7.66 (m, 6H),

7.13–7.33 (m, 4H), 5.63 (s, 2H), 4.39 (d, 2H), 4.10–4.25 (m, 2H), 3.63 (s, 2H), 2.47–2.60 (m, 2H), 2.20–2.35 (m, 1H), 1.95–2.15 (m, 1H), 1.45 (s, 9H); Elemental analysis calcd for $C_{32}H_{34}O_7N_2 \cdot 1/2\ H_2O$: C, 67.71; H, 6.21; N, 4.93. Found: C, 67.67; H, 6.14; N, 4.91.

***N*-*t*-Boc-4-aminomethylbenzyl alcohol.**[36] In a 2-L, three-necked, round-bottomed flask equipped with a heating mantle, an overhead stirrer bearing a two-bladed propeller, a reflux condenser with a drying tube packed with Drierite, were placed 1 L of anhydrous dioxane and THF (1/1) and 18.7 g (0.5 mol) of lithium aluminum hydride ($LiAlH_4$). The suspension is heated to boil and refluxed for 15 min with stirring and cooled to rt with stirring. Powdered 4-aminomethylbenzoic acid (22.65 g, 150 mmol) was added in small portions (less than 1 g) to the solution at such a rate as to maintain reflux with stirring. After adding all the powder, the solution was refluxing for 10 h with stirring. After cooling to rt, ethyl acetate (60 mL) was added drop by drop from a dropping funnel with a pressure-equalization arm, then water (20 mL), 15% sodium hydroxide (50 mL) and water (20 mL) were added drop by drop with stirring. The mixture was filtered and the filter cake was washed with THF and ethyl alcohol. The organic filtrates were combined and evaporated. Then the residue was dissolved in 300 mL of dioxane and water (1/1). Di-*t*-butyl dicarbonate (32.7 g, 150 mmol) was added. The solution was stirred for 10 h at rt, then most of the dioxane was evaporated and the residue was extracted with ethyl acetate. The organic layer was washed with 5% (w/v) $NaHCO_3$, water, 5% (w/v) citric acid, and water, dried over $MgSO_4$ and evaporated. The solid was recrystallized from ethyl acetate and hexanes: Yield 24.82 g (69.7%); mp 97–98 °C; ^{1}H NMR (DMSO-d_6) δ 7.35 (t, 1H), 7.23 (d, 2H), 7.15 (d, 2H), 5.05–5.15 (br, 1H), 4.44 (s, 2H), 4.08 (d, 2H), 1.38 (s, 9H); Elemental analysis calcd for $C_{13}H_{19}O_3N$: C, 65.80; H, 8.07; N, 5.90. Found: C, 65.79; H, 8.08; N, 5.89.

***N*-Boc-4-aminomethylbenzyl chloride.**[37] *N*-Boc-4-aminomethylbenzyl alcohol (4.86 g, 20 mmol) was dissolved in DCM (20 mL), and Ph_3P (7.84 g, 30 mmol) and CCl_4 (15 mL) was added. The mixture was stirred for 24 h at rt. The solvents were evaporated. The mixture was separated by silica gel flash chromatography (eluent: $CHCl_3$/hexanes, 2/1): Yield 3.9 g (75%); mp 87–89 °C; ^{1}H NMR ($CDCl_3$) δ 7.26–7.40 (two d, 4H), 4.8–4.9 (br, 1H) 4.58 (s, 2H), 4.31 (d, 2H), 1.46 (s, 9H).

***N*-Boc-4-aminomethylbenzyl cyanide.** Sodium cyanide (2.0 g, 40 mmol) was dissolved in water (40 mL). A solution of *N*-Boc-4-aminomethylbenzyl chloride (3.1 g, 11.5 mol) in ethanol (50 mL) was added into the aqueous solution of sodium cyanide drop by drop, then the mixture was refluxed for 5 h and cooled to rt. The ethanol was evaporated and the residue was extracted with ethyl acetate. The organic layer was then washed with water and dried over Na_2SO_4, then evaporated. The residue was recrystallized from ether and hexanes: Yield 2.41 g (83.1%); ^{1}H NMR ($CDCl_3$) δ 7.30 (s, 4H), 4.80–4.90 (br, 1H), 4.32 (d, 2H), 3.75 (s, 2H), 1.46 (s, 9H).

***N*-Fmoc-4-(aminomethyl)phenylacetic acid (Fmoc-AMPA-OH).** *N*-Boc-4-(aminomethyl)benzyl cyanide (2.27 g, 9.0 mmol) was placed in a 250-mL round-bottomed flask. Concentrated HCl (36%, 60 mL) was added and the mixture was refluxed for 4 h and then evaporated. The residue was dried under vacuum for 2 days. The solid was then dissolved in 50 mL water. DIEA (3.9 g, 30 mmol) was added and a solution of Fmoc-OSu (2.87 g, 8.5 mmol) in CH_3CN was added drop by drop over 15 min. The mixture was stirred for 1 h. The acetonitrile was evaporated and water (50 mL) was added. The aqueous solution was extracted with diethyl ether. HCl (2 N, 60 mL) was added into the aqueous layer and the mixture was filtered, and the solid washed with water and dried under vacuum. The crude product was recrystallized from ethanol and diethyl ether: Yield 2.57 g (78.0%); mp 191–193 °C; ^{1}H NMR (DMSO-d_6) δ 12.15 (s, 1H), 7.8–8.0 (m, 3H), 7.72 (d, 2H), 7.3–7.5 (m, 4H), 7.1–7.3 (m, 4H), 4.35 (d, 2H), 4.23 (t, 1H), 4.16 (d, 2H), 3.55 (s, 2H); Elemental analysis calcd for $C_{24}H_{21}O_4N$: C, 74.40; H, 5.46; N, 3.61. Found: C, 73.93; H, 5.22; N, 3.46.

***N*$^{\alpha}$-*t*-Boc-(L)-Dap(*N*-Fmoc-AMPA)-OH (Boc-Dap[Fmoc-AMPA]-OH).** *N*-Fmoc-4-(aminomethyl)phenylacetic acid (Fmoc-AMPA-OH) (2.32 g, 6.0 mmol) was dissolved in anhydrous dioxane and ethyl acetate (100 mL, 1/1). *N*-Hydroxysuccinimide (0.81 g, 7.0 mmol) and DCC (1.34 g, 6.5 mmol) were added. The mixture was stirred for 20 h at rt, and then the DCU was removed by filtration. The solvents were evaporated and the crude active ester product (Fmoc-AMPA-OSu) was used without further purification. Boc-(L)-Dap-OH (1.43 g, 7 mmol) was dissolved in 2.5% (w/v) $NaHCO_3$ (60 mL). A solution of the Fmoc-AMPA-OSu in dioxane (60 mL) was added, and this mixture was stirred for 10 h at rt. The dioxane was then evaporated, and the residue was acidified with 5% (w/v) citric acid and extracted with DCM. The organic layer was washed with citric acid and water, dried over Na_2SO_4, and evaporated. The crude product was then purified by silica gel flash chromatography (eluent: $CHCl_3$/MeOH/AcOH). The eluent was evaporated and the residue was dissolved in DCM (500 mL). This solution was washed with water, dried over Na_2SO_4, and evaporated: Yield 2.41 g (70%); mp sublimes at 110 °C; ^{1}H NMR (DMSO-d_6) δ 12.3 (s, 1H), 8.1 (br, 1H), 7.87 (d, 2H), 7.76–7.86 (br, 1H), 7.7 (d, 2H), 7.23–7.46 (m, 4H), 7.14 (s, 4H), 6.95 (d, 1H), 4.30 (d, 2H) , 3.95–4.25 (m, 4H), 3.38 (s, 2H), 3.25–3.32 (m, 2H), 1.37 (s, 9H); Elemental analysis calcd for $C_{32}H_{35}O_7N_3$: C, 67.00; H, 6.15; N, 7.32. Found: C, 66.53; H, 6.15; N, 7.09.

Peptide-ABA and peptide-APA. These two peptides were synthesized following the method outlined in Scheme 1. To attach the C-terminal Gln residue to the hydroxylmethyl resin, the resin (3.0 g, 1.8 mequiv) was swollen in 50 mL of DCM and cooled to 0 °C, then Boc-(L)-Gln-OH (1.0 mmol), DCC (1.1 mmol) and DMAP (0.1 mmol) were added. The suspension was shaken for 30 min at 0 °C and for 8 h at rt. The resin was then washed with DCM (×2), DMF (×2), EtOH (×2), DMF (×1), MeOH (×2) and DCM (×3). The substitution

level of the first amino acid was determined by picric acid titration (0.230 mequiv/g for peptide-ABA; 0.259 mequiv/g for peptide-APA). The remaining free hydroxyl groups on the resin were blocked by acetylation overnight in DCM, using acetic anhydride (20 equiv) and DIEA (10 equiv). The peptidyl resin was deprotected and washed according to standard solid-phase synthesis procedures, using Boc/Benzyl chemistry.[38] The amino acid derivatives used in nonbridging positions were N^{α}-Boc-(L)-Gln, N^{α}-Boc-(L)-Glu(OBzl)-OH, N^{α}-Boc-(L)-Leu, and N^{α}-Boc-(L)-Lys(2Cl-Z)-OH. Peptide-chain elongations were performed using three equivalents each of the Boc-amino acid derivative, HBTU,[42] HOBt[43] and DIEA, in DMF and DCM (2/1, v/v). Typically, coupling reactions were complete in under 2 h, as judged by the Kaiser ninhydrin assay.[38] The orthogonal-protecting groups, Fmoc and OFm, on the side chains of the bridging residues were deprotected using 20% (v/v) piperidine in DMF for 20 min. The cyclization of the side chains was carried out for about 10 h using 1.1 equiv each of HBTU, HOBt, and DIEA in DMF and DCM (2/1, v/v), and was followed by the Kaiser test.[38] The fully protected peptidyl-resin (300 mg) was cleaved with anhydrous HF/anisole/DMS (10/1/1, v/v/v) for 1 h at 0 °C.[38,39] After diethyl ether precipitation and washing, the crude peptides were extracted by 10% (v/v) acetic acid, and lyophilized. Crude peptides with high purity were obtained. The crude peptides were purified to apparent homogeneity by RP-HPLC. Amino acid analysis of peptide-ABA gave: Glx (5) 4.82, Leu (4) 4.00, Dab (1) 0.80, Lys (4) 3.85. MS: 1830 ± 1 (calcd 1829.1 for $[M+H]^+$ average mass). Amino acid analysis of peptide-APA gave: Glx (5) 4.95, Leu (4) 4.00, Dap (1) 0.85, Lys (4) 3.90. MS: 1829 ± 1 (calcd 1829.1 for $[M+H]^+$ average mass).

Peptide-AMBA and peptide-AMPA. These two peptides were synthesized following the method outlined in Scheme 2. The C-terminal glutamine residue was first attached to Merrifield resin using the cesium salt of Boc-(L)-Gln-OH, as follows. Boc-(L)-Gln-OH (1.1 mmol) was dissolved in 10 mL of ethanol and $CeHCO_3$ (1.1 mmol) in 2 mL of water was added. The solvent was evaporated. Anhydrous ethanol was added and evaporated again three times to remove all the water. The residue was then dried under vacuum over P_2O_5 for 2 days. The dried product was dissolved in DMF (50 mL) and Merrifield resin (3 g, 0.64 mequiv/g) was added. The mixture was shaken for 12 h at 50 °C, then the substituted resin was washed with DMF (×2), water (×2), DMF (×1), DMF/water (9/1, v/v) (×2), DMF (×1), ethanol (×2) and DCM (×3). Boc-(L)-Gln substitution levels were determined by picric acid titration[38] (0.34 mequiv/g for peptide-AMPA, and 0.19 mequiv/g for peptide-AMBA). Peptide-chain elongation and cyclization procedures followed those of peptide-ABA and peptide-APA. Amino acid analysis of peptide-AMPA gave: Asx (1) 1.04, Glx (4) 4.13, Leu (4) 4.00, Dap (1) 0.91, Lys (4) 4.01. MS 1829 ± 1 (calcd 1829.1 for $[M+H]^+$ average mass). Amino acid analysis of peptide-AMBA gave: Asx (1) 1.14, Glx (4) 3.85, Leu (4) 4.00, Dab (1) 0.92, Lys (4) 3.70. MS: 1828 ± 1 (calcd 1829.1 for $[M+H]^+$ average mass).

Circular dichroism spectropolarimetry

CD spectra were recorded on an Aviv Model 62ds spectropolarimeter fitted with a Peltier temperature controller. In all cases, peptide concentrations were determined by quantitative amino acid analysis, and mean residue ellipticities [θ] were calculated based on the number of amino acid residues constituting the peptide backbone ($n = 14$), without accounting for the bridging structures. Phosphate buffers were prepared by titrating the appropriate concentration of NaH_2PO_4 in distilled, deionized H_2O to pH 7.0, at rt, using NaOH. Peptide spectra were recorded under temperature control in 0.1 cm, 0.5 cm or 1.0 cm pathlength cells, depending on the peptide concentration, using a 1.0 nm step size, a 1.5 nm bandwidth and a 1.0 s averaging time. Melting and annealing studies were performed by monitoring ellipticity at 222 nm, using a bandwidth of 2.0 nm and an averaging time of 30 s, as the temperature was changed from 0 °C to 90 °C in 4 °C increments (peptide 2-2), or 3 °C increments (all other peptides), over a period of approximately 4 h. Quantitative analysis of peptide spectra by least-squares fitting to linear combinations of the standard spectra of Brahms and Brahms[24] or Perczel et al.[25] were performed using the program LINCOMB,[25] which constrains the fractional contributions of the standard spectra in the best-fit spectrum to sum to 100%.

Acknowledgement

This research was supported by NIH grant DA 04197.

References

1. Kaiser, E. T.; Kezdy, F. J. *Science* **1984**, *223*, 249.
2. Taylor, J. W.; Kaiser, E. T. *Pharmacol. Rev.* **1986**, *38*, 291.
3. Ellenberger, T.; Fass, D.; Arnaud, M.; Harrison, S. C. *Genes Dev.* **1994**, *8*, 970.
4. Dill, K. A. *Biochemistry* **1985**, *24*, 1501.
5. Felix, A. M.; Heimer, E. P.; Wang, C. T.; Lambros, T. J.; Fournier, A.; Mowles, T. F.; Maines, S.; Campbell, R. M.; Wegrzynski, B. B.; Toome, V.; Fry, D.; Madison, V. S. *Int. J. Pept. Protein Res.* **1988**, *32*, 441.
6. Kapurniotu, A.; Taylor, J. W. *J. Med. Chem.* **1995**, *38*, 836.
7. Chorev, M.; Epand, R. F.; Rosenblatt, M.; Caulfield, M. P.; Epand, R. M. *Int. J. Pept. Protein Res.* **1993**, *42*, 342.
8. Bouvier, M.; Taylor, J. W. *J. Med. Chem.* **1992**, *35*, 1145.
9. Wu, B. Y.; Gaffney, B. L.; Jones, R. A.; Taylor, J. W. In *Proc. 14th Amer. Peptide Symp.; Peptides: Chemistry, Structure and Biology*; Kaumaya, P. T. P.; Hodges, R. S., Eds.; Mayflower Scientific: Kingswinford, England, 1996; pp 265–266.
10. Wu, B. Y. Ph.D. Thesis, Rutgers University at New Brunswick, 1996.
11. Sueki, M.; Lee, S.; Powers, S. P.; Denton, J. B.; Konishi, Y.; Scheraga, H. A. *Macromolecules* **1984**, *30*, 121.
12. Taylor, J. W.; Guo, G.; Wu, B.; Yu, C.; Zhang, M.; Zhang, W. In *Peptidomimetics & Small Molecule Design*; International Business Corporation Library Series: Southborough, MA, 1997; publication #984, pp 87–120.
13. Osapay, G.; Gulyas, J.; Profit, A. A.; Gulyas, E. S.; Taylor, J. In *Proc. 12th Amer. Peptide Symp.; Peptides: Chemistry and Biology*; Smith, J. A.; Rivier, J. E., Eds.; ESCOM Science Publishers B. V.: Leiden, 1992; pp 239–240.

14. Osapay, G.; Taylor, J. W. *J. Am. Chem. Soc.* **1992**, *114*, 6966.
15. Luo, P.; Braddock, D. T.; Subramanian, R. M.; Meredith, S. C.; Lynn, D. G. *Biochemistry* **1994**, *33*, 12367.
16. Bracken, C.; Gulyas, J.; Taylor, J. W.; Baum, J. *J. Am. Chem. Soc.* **1994**, *116*, 6431.
17. Zhang, M.; Wu, B.; Baum, J.; Taylor, J. W. In *Proc. 15th Am. Peptide Symp.*; Tam, J. P.; Kaumaya, P. T. P., Eds.; Kluwer Academic Publishers, in press.
18. Jackson, D. Y.; King, D. S.; Chmielewski, J.; Singh, S.; Schultz, P. G. *J. Am. Chem. Soc.* **1991**, *113*, 931.
19. Fairman, R.; Anthony-Cahill, S. J.; DeGrado, W. F.; *J. Am. Chem. Soc.* **1992**, *114*, 5458.
20. Phelan, J. C.; Skelton, N. J.; Braisted, A. C.; McDowell, R. S. *J. Am. Chem. Soc.* **1997**, *119*, 455.
21. Yu, C.; Taylor, J. W. *Tetrahedron Lett.* **1996**, *37*, 1731.
22. Story, S. C.; Aldrich, J. V. *Int. J. Peptide Protein Res.* **1994**, *43*, 292.
23. Chen, Y.-H.; Yang, J. T.; Chau, K. H. *Biochemistry* **1974**, *13*, 3350.
24. Brahms, S.; Brahms, J. *J. Mol. Biol.* **1980**, *138*, 149.
25. Perczel, A.; Park, P. K.; Fasman, G. D. *Anal. Biochem.* **1992**, *203*, 83.
26. Luo, P.; Baldwin, R. L. *Biochemistry* **1997**, *36*, 8413.
27. Zhou, N. E.; Mant, C. T.; Hodges, R. S. *Peptide Res.* **1990**, *3*, 8.
28. Krause, E.; Beyermann, M.; Dathe, M.; Wenschuh, H.; Rothemund, S.; Bienert, M. In *Proc. 13th Amer. Peptide Symp.; Peptides: Chemistry, Structure and Biology*; Hodges, R. S.; Smith, J. A., Eds.; ESCOM Science Publishers B.V.: Leiden, 1994; pp 247–248.
29. Purcell, A. W.; Hearn, M. T. W.; Aguilar, M. I. In *Proc. 13th Amer. Peptide Symp.; Peptides: Chemistry, Structure and Biology*; Hodges, R. S.; Smith, J. A., Eds.; ESCOM Science Publishers B. V.: Leiden, 1994; pp 769–771.
30. Kapurniotu, A.; Taylor, J. W. *Tetrahedron Lett.* **1993**, *34*, 7031.
31. Ten Kortenaar, P. B. W.; Van Dijk, B. G.; Peeters, J. M.; Raaben, B. J.; Adams P. J. H. M.; Tesser, G. I. *Int. J. Peptide Protein Res.* **1986**, *27*, 398.
32. Radhakrishna, A. S.; Parham, M. E.; Riggs, R. M.; London, G. M. *J. Org. Chem.* **1979**, *44*, 1746.
33. Waki, M.; Kitajima, Y.; Izumiya, N. *Synthesis* **1981**, *1981*, 266.
34. Bolin, D. R.; Wang, C.-T.; Felix, A. M. *Organic Preparations and Procedures International* **1989**, *21*, 67.
35. Bodanszky, M.; Bodanszky, A. In *The Practice of Peptide Synthesis*; Springer–Verlag: New York, 1984; pp 105–106.
36. Enders, D.; Fey, P.; Kipphardt, H. *Org. Synth.* **1987**, *65*, 173.
37. Weiss, R. G.; Snyder, E. I. *J. Org. Chem.* **1971**, *36*, 403.
38. Stewart, J. M.; Young, J. D. In *Solid-Phase Peptide Synthesis*; Pierce Chemical Co.: Rockford, IL, 1984; pp 53–123.
39. Tam, J. P.; Heath, W. F.; Merrifield, R. B. *J. Am. Chem. Soc.* **1983**, *105*, 6442.
40. Bodanszky, M.; Bodanszky, A. In *The Practice of Peptide Synthesis*; Springer–Verlag: New York, 1984; p 20.
41. Lapatsanis, L.; Milias, G.; Froussios, K.; Kolovos, M. *Synthesis* **1983**, *1983*, 671.
42. Dourtoglou, V.; Gross, B. *Synthesis* **1984**, *1984*, 572.
43. König, W.; Geiger, R. *Chem. Ber.* **1973**, *106*, 3626.